

Analysis of two-dimensional thin structures (from micro- to nano-scales) using the boundary element method

J. F. Luo, Y. J. Liu, E. J. Berger

404

Abstract In this paper, the boundary element method (BEM) based on elasticity theory is developed for two-dimensional (2-D) thin structures with the thickness to length ratio in the micro (10^{-6}) or nano (10^{-9}) scales. An efficient analytical method is developed to deal with the nearly-singular integrals in the boundary integral equation (BIE) for 2-D thin structures. The nearly-singular integrals, which are line integrals for 2-D problems and arise when two boundary curves are close to each other, are transformed into function evaluations at the two end points of the element of integration. In addition, a new nonlinear coordinate transformation is developed for nearly weakly-singular integrals to further increase the numerical accuracy. For the test problems studied, very promising results are obtained when the thickness to length ratio is in the orders of 10^{-6} to 10^{-9} , which is sufficient for modeling most thin structures in the micro- or nano-scales. The developed method can be applied readily to model layered coatings, thin films or other layered structures to analyze contact stresses, interfacial cracks, thermal effects and nonlinear deformations.

1

Introduction

With the advances in materials science and manufacturing, more and more thin structures, such as various thin films in electronic devices, sensors and actuators in smart materials, and coatings on machine components, are being designed and utilized in many industries. For example, in recent years the use of coatings on machine elements for

wear resistance, corrosion inhibition, or friction reduction has become widespread. Coatings can provide a durable and low cost solution to many machine element performance problems, as described in (Subramanian and Strafford 1993). However, the widespread experimental research in thin films and coatings (Bhushan and Gupta 1991) – everything from thin film/coating and substrate interface strength and adhesion, to deposition rate and resultant hardness – underlies a general lack of modeling efforts which can accurately and efficiently predict thin film and coating performance, including subsurface stresses and fatigue life. Robust models for thin film and coating performance are crucial for accurate design and analysis of systems containing such thin structures. Yet the development of modeling and analysis tools for these very relevant problems has lagged the state-of-the-art experimental and technological advances. The primary obstacles to the development of robust and accurate thin film and coating analysis tools have been difficult computational issues associated with the general class of thin structures.

For computational models of thin structures or thin shapes in structures, two numerical methods can be employed, namely, the finite element method (FEM) and the boundary element method (BEM). In the last three decades, the FEM based on plate and shell theories has been a successful tool for the analysis of 3-D thin structures such as plates, shells and layered composite structures to study their deformation and stress in the macro-scale. However, most plate and shell theories are based on various assumptions about the geometry, loading and deformation of the structure, and therefore the accuracy and reliability of the FEM for thin structures in the micro- or nano-scales are in doubt. This is especially true for the stress analysis of thin structures since plate and shell models can not predict the normal stresses (contact stresses) accurately. The BEM based on the elasticity theory and boundary integral equation formulation (see, for example (Banerjee 1994)), is in general more accurate in stress analysis of structures. This accuracy will be maintained in the analysis of thin structures as well, if the BEM is implemented correctly to deal with the difficulties associated with thin structures.

There have been two major concerns in applying the BEM to thin structures. The first concern is whether or not the conventional boundary integral equation (CBIE) for elasticity problems can be applied to thin structures. It is well known in the BIE/BEM literature that the CBIE will degenerate when it is applied to cracks or thin voids in structures because of the closeness of the two crack sur-

Communicated by T. A. Cruse and S. N. Atluri, 10 August 1998

J. F. Luo, Y. J. Liu, E. J. Berger
Department of Mechanical,
Industrial and Nuclear Engineering, P.O. Box 210072,
University of Cincinnati, Cincinnati,
Ohio 45221-0072

Correspondence to: Y. J. Liu

The authors would like to thank Dr. Leonard Gray at Oak Ridge National Laboratory for discussions on the subject of nearly-singular integrals in 2-D BEM. The second and third authors (Y.J.L. and E.J.B.) would like to acknowledge the research startup fund provided by the University of Cincinnati. The second author (Y.J.L.) acknowledges gratefully the partial support by NSF grant CMS-9734949.

faces, see, e.g. References (Cruse 1988; Krishnasamy, Rizzo and Liu 1994). One of the remedies to such degeneracy in the CBIE for crack-like problems (*exterior-like* problems), is to employ the hypersingular boundary integral equation (HBIE), or the traction BIE, see, e.g. (Gray, Martha and Ingrassia 1990; Krishnasamy, Rizzo and Rudolphi 1991; Cruse 1996; Liu and Rizzo 1997). Does this degeneracy occur when the CBIE is applied to thin structures (*interior-like* problems), such as thin shells? It was not clear in the BEM literature and the BEM based on elasticity had been avoided in analyzing thin shell-like structures for a long time due to this concern. Recently, it was shown in (Liu 1998), both analytically and numerically, that the CBIE will not degenerate when it is applied to thin shell-like structures, contrary to the case of crack-like problems. Thus the degeneracy issue should no longer be a concern when the CBIE is applied to thin structures, once the second concern, i.e., the numerical difficulty, is addressed.

The numerical difficulty in the BIE is the nearly-singular integrals which arise in both crack-like and thin-structure problems. The integrals in BIE, which determine the influence matrices, contain singular kernels of the order $O(1/r)$ and $O(\ln r)$ in 2-D elasticity case, where r is the distance between the source point and the integration point on the boundary element. When the source point is very close to, but not on the element ($0 < e \ll 1$, with e being the distance from the source point to the element of integration), although the kernels are regular in the mathematical sense, the values of the kernels change rapidly in the neighborhood of the source point. The standard Gauss-quadrature is no longer practical in this case since a large number of integration points are needed in order to achieve the required accuracy. In the last two decades, numerous research works have been published on this subject in the BEM literature. Most of the work has been focused on the numerical approaches, such as subdivisions of the element of integration, adaptive integration schemes and so on. However, most of these earlier methods are either inefficient or can not provide accurate results when the ratio of the distance e to the element size is smaller than 10^{-2} . They are not very useful in dealing with thin structures, such as thin films or coatings, with the thickness to length ratio in the micro- or nano-scales.

Detailed studies on the behaviors of the nearly-singular integrals and comprehensive reviews of the earlier work in this regard can be found in (Cruse and Aithal 1993) and (Huang and Cruse 1993). In (Cruse and Aithal 1993), a semi-analytical approach is developed using Taylor expansions for the kernel functions. The singular part of the kernel is integrated analytically and the remaining part is computed using lower-order Gaussian integration. Significant improvement in accuracy in computing the nearly-singular integrals is achieved using this approach, as demonstrated by several numerical examples of 3-D thin structures with the thickness to length (or element size) ratio in the 10^{-3} range. In (Huang and Cruse 1993), a new formulation is developed for computing the nearly-singular integrals in the BEM for 3-D elastostatic problems. A coordinate transformation, which can smooth out the variation of the nearly-singular kernels, is introduced in

the integral in the radial direction (which has the singular part) in the local polar coordinates. For the test case using a 1-D integral representing this polar integral, it is shown that the nearly-singular integrals can be computed almost exactly with only a few Gaussian points. Although no applications of this new approach to thin-structure problems were reported in (Huang and Cruse 1993), this approach has the potential to provide accurate results for thin structures with arbitrary thickness to length ratios, possibly in the micro- or nano-scales. An alternative to dealing directly with the singular or even hypersingular integrals in the BEM is to employ a regularized algorithms, see, for examples (Chien, Rajiyah and Atluri 1991) and (Richardson, Cruse and Huang 1997). In this approach, simple solutions or modes of the governing equations are used to regularize the singular or hypersingular integrals so that the singularities are reduced and thus efficient numerical algorithms can be established. Very successful numerical results have been reported in (Chien, Rajiyah and Atluri 1991) and (Richardson, Cruse and Huang 1997) for 2-D elasticity problems using the hypersingular BIEs. However, whether or not this approach will work for thin structures with nearly singular integrals, in which the source point is close but off the boundary, will need further investigation.

Another efficient and accurate approaches to deal with the nearly-singular integrals in the BEM for 3-D problems is to transform these (surface) integrals to line integrals analytically and then carry out the numerical integration for these line integrals (Liu, Zhang and Rizzo 1993; Krishnasamy, Rizzo and Liu 1994; Liu and Rizzo 1997; Liu 1998). It has been found out that using this line integral approach is not only accurate, but also very efficient. The CPU time for computing these line integrals is only a fraction of the CPU time used by subdividing the surface elements and employing a large number of Gaussian points on each sub-regions.

With the degeneracy issue for the CBIE in thin structure problems having been clarified and the nearly-singular integrals been dealt with accurately and efficiently, it is believed that the boundary element method can now be applied to a new and wide range of problems in engineering, including simulations of thin shell-like structures, composite materials in the micro-scale, and thin-film or thin-layer structures in the micro- or nano-scales.

In this paper, the BEM based on the elasticity theory is developed for 2-D thin structures with the thickness to length ratio in the micro (10^{-6}) or nano (10^{-9}) range. Adopting the same approach using the line integrals as in the case of 3-D BIEs, an efficient method is developed to deal with the nearly-singular integrals in the BIE for 2-D thin structures. The nearly-singular integrals (line integrals for 2-D problems) are transformed into function evaluations at the two end points of the element of integration. In addition, a new nonlinear coordinate transformation is developed for nearly weakly-singular integrals to further increase the numerical accuracy. For the test problems studied, very promising results are obtained when the thickness to length ratio is in the orders of 10^{-6} to 10^{-9} , which is sufficient for modeling most thin structures in the micro- or nano-scales.

The nearly-singular integrals in 2-D elasticity

We consider the following conventional boundary integral equation for 2-D elastostatic problems (the index notation is used) (Mukherjee 1982; Cruse 1988; Banerjee 1994),

$$C_{ij}(P_0)u_j(P_0) = \int_L [U_{ij}(P, P_0)t_j(P) - T_{ij}(P, P_0)u_j(P)] dL(P), \quad \forall P_0 \in L \tag{1}$$

in which u_i and t_i are the displacement and traction fields, respectively, U_{ij} and T_{ij} the displacement and traction kernel (Kelvin's solution), respectively, P the field point and P_0 the source point, and L the boundary of the structure, Fig. 1. $C_{ij}(P_0)$ is a coefficient matrix depending on the smoothness of the curve L at the source point P_0 (for example, $C_{ij}(P_0) = 1/2\delta_{ij}$ for smooth curves, where δ_{ij} is the Kronecker delta). The BIE (1) will be discretized using the boundary elements (line segments for 2-D problems) where analytical or numerical integrations will be carried out, leading to a system of linear equations for unknown boundary variables at a finite number of nodes.

The two kernel functions in Eq. (1), $U_{ij}(P, P_0)$ and $T_{ij}(P, P_0)$, are given as follows for 2-D plane strain problems:

$$U_{ij}(P, P_0) = \frac{1}{8\pi\mu(1-\nu)} \left[(3-4\nu)\delta_{ij} \ln\left(\frac{1}{r}\right) + \frac{\partial r}{\partial x_i} \frac{\partial r}{\partial x_j} \right], \tag{2}$$

$$T_{ij}(P, P_0) = -\frac{1}{4\pi(1-\nu)r} \left\{ \frac{\partial r}{\partial n} \left[(1-2\nu)\delta_{ij} + 2\frac{\partial r}{\partial x_i} \frac{\partial r}{\partial x_j} \right] + (1-2\nu) \left(\frac{\partial r}{\partial x_j} n_i - \frac{\partial r}{\partial x_i} n_j \right) \right\}, \tag{3}$$

where μ is the shear modulus, ν the Poisson's ratio, r the distance from source P_0 to the field point P , and n_i the directional cosines of the normal n . Notice that the displacement kernel U_{ij} and traction kernel T_{ij} contain the terms $\ln(1/r)$ and $1/r$, respectively, which are singular terms when the distance r approaches zero. Because of the existence of these two singular terms, the integrals on a typical element ΔL

$$\int_{\Delta L} U_{ij}(P, P_0)t_j(P) dL(P) \tag{4}$$

and

$$\int_{\Delta L} T_{ij}(P, P_0)u_j(P) dL(P) \tag{5}$$

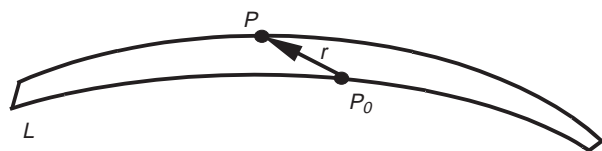


Fig. 1. Sketch of a 2-D thin structure with boundary L

are called *weakly*- (the Logarithm type) and *strongly*- (the Cauchy principle value (CPV) type) singular integrals, respectively, when P_0 is on the element ΔL . When the source is not on the element but very close to it ($0 < r \ll 1$), the kernel is regular in the mathematical sense. However, the values of the kernels change rapidly in the neighborhood of the source point and the standard Gauss-quadrature becomes impractical since a very large number of integration points is needed in order to achieve the required accuracy. In such situations, the integrals (4) and (5) are called *nearly weakly*- and *strongly*-singular integrals, respectively (or simply, *nearly-singular integrals*). In the modeling of thin structures in the micro- or nano-scales by the BEM, the most important research efforts involve finding efficient and accurate ways to deal with these nearly-singular integrals. In the following, we will discuss how to evaluate them by singularity subtraction and nonlinear coordinate transformation methods for 2-D thin structure problems.

2.1 Regularize the nearly-singular integral by singularity subtraction

A method similar to that developed in (Liu, Zhang and Rizzo 1993; Krishnasamy, Rizzo and Liu 1994; Liu 1998) for 3-D thin structures is used in this paper to regularize or weaken the nearly-singular integral given in (5) in the 2-D case. By subtracting and adding back a term in the following manner, the nearly-singular integral (5) can be rewritten as:

$$\begin{aligned} & \int_{\Delta L} T_{ij}(P, P_0)u_j(P) dL(P) \\ &= \int_{\Delta L} T_{ij}(P, P_0)[u_j(P) - u_j(P'_0)] dL(P) \\ & \quad + u_j(P'_0) \int_{\Delta L} T_{ij}(P, P_0) dL(P), \end{aligned} \tag{6}$$

where ΔL is the line segment under consideration, P'_0 is the closest point on ΔL to P_0 (an image point of P_0 on ΔL), Fig. 2. As $P \rightarrow P'_0$, the term $u_j(P) - u_j(P'_0)$ has the order of $O(r')$ (see Fig. 2 for r'). Then the order of the first integral on the right hand side is reduced to $O(r')/O(r)$. This integral is a nearly weakly-singular integral when the distance e (Fig. 2) is very small. We will discuss how to evaluate it accurately by a nonlinear coordinate transformation in the next section. Now, we focus on the evaluation of the last integral in (6) by an analytical method.

Considering the local polar coordinate with the origin at the source point P_0 , Fig. 3, we have the following relations:

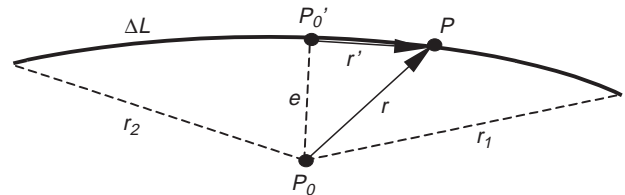


Fig. 2. Source point P_0 near the line ΔL of integration

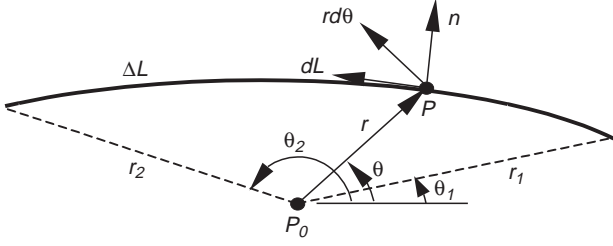


Fig. 3. The local polar coordinate system

$$\frac{\partial r}{\partial x_i} = \delta_{1i} \cos \theta + \delta_{2i} \sin \theta, \quad (7)$$

$$\frac{\partial r}{\partial n} = \frac{rd\theta}{dL}. \quad (8)$$

Applying (7) and (8) in (3), we can derive the following expression:

$$\begin{aligned} & \int_{\Delta L} T_{ij}(P, P_0) dL(P) \\ &= C_1 \left\{ C_2 \int_{\Delta L} \frac{1}{r} \frac{\partial r}{\partial n} \delta_{ij} dL + 2 \int_{\Delta L} \frac{1}{r} \frac{\partial r}{\partial n} \frac{\partial r}{\partial x_i} \frac{\partial r}{\partial x_j} dL \right. \\ & \quad \left. + C_2 \int_{\Delta L} \frac{1}{r} \left(\frac{\partial r}{\partial x_j} n_i - \frac{\partial r}{\partial x_i} n_j \right) dL \right\} \\ &= C_1 \left\{ C_2 \int_{\Delta L} \delta_{ij} d\theta + 2 \int_{\Delta L} \frac{\partial r}{\partial x_i} \frac{\partial r}{\partial x_j} d\theta \right. \\ & \quad \left. + C_2 \int_{\Delta L} \left(\frac{\partial \ln(r)}{\partial x_j} n_i - \frac{\partial \ln(r)}{\partial x_i} n_j \right) dL \right\} \\ &= C_1 \left\{ C_2 \delta_{ij} \theta \Big|_{\theta_1}^{\theta_2} + 2 \int_{\Delta L} [\delta_{1i} \delta_{1j} \cos^2 \theta + \delta_{2i} \delta_{2j} \sin^2 \theta \right. \\ & \quad \left. + (\delta_{1i} \delta_{2j} + \delta_{2i} \delta_{1j}) \sin \theta \cos \theta] d\theta \right. \\ & \quad \left. + C_2 \int_{\Delta L} \left(\frac{\partial \ln(r)}{\partial x_j} n_i - \frac{\partial \ln(r)}{\partial x_i} n_j \right) dL \right\} \\ &= C_1 \left\{ C_2 \delta_{ij} \theta + \delta_{1i} \delta_{1j} (\theta + \frac{1}{2} \sin 2\theta) \right. \\ & \quad \left. - \frac{1}{2} (\delta_{1i} \delta_{2j} + \delta_{2i} \delta_{1j}) \cos 2\theta + \delta_{2i} \delta_{2j} (\theta - \frac{1}{2} \sin 2\theta) \right\} \Big|_{\theta_1}^{\theta_2} \\ & \quad + C_1 C_2 \int_{\Delta L} \left(\frac{\partial \ln(r)}{\partial x_j} n_i - \frac{\partial \ln(r)}{\partial x_i} n_j \right) dL \quad (9) \end{aligned}$$

where $C_1 = -1/4\pi(1 - \nu)$ and $C_2 = 1 - 2\nu$. Using the Stokes' theorem (Kreyszig 1972) to evaluate the last integral in Eq. (9), we obtain

$$\int_{\Delta L} \left(\frac{\partial \ln(r)}{\partial x_j} n_i - \frac{\partial \ln(r)}{\partial x_i} n_j \right) dL = (e_{1i} e_{2j} - e_{2i} e_{1j}) \ln r \Big|_{r_1}^{r_2}, \quad (10)$$

where e_{ij} is the permutation tensor. Substitution of (10) into (9) yields the final expression:

$$\begin{aligned} \int_{\Delta L} T_{ij}(P, P_0) dL(P) &= C_1 C_2 (e_{1i} e_{2j} - e_{2i} e_{1j}) \ln r \Big|_{r_1}^{r_2} \\ & \quad + C_1 \left\{ C_2 \delta_{ij} \theta + \delta_{1i} \delta_{1j} (\theta + \frac{1}{2} \sin 2\theta) \right. \\ & \quad \left. - \frac{1}{2} (\delta_{1i} \delta_{2j} + \delta_{2i} \delta_{1j}) \cos 2\theta + \delta_{2i} \delta_{2j} (\theta - \frac{1}{2} \sin 2\theta) \right\} \Big|_{\theta_1}^{\theta_2} \quad (11) \end{aligned}$$

Thus, we have converted the last integral in (6) to function evaluations at the two end points of the element ΔL , as given in (11). It is interesting to note that this integral does not depend on the integration path ΔL . This means that, no matter what kind of element is applied, the last integral in (6) is only determined by locations of the source point P_0 and the two end points of the element ΔL . Obviously, there is no difficulty at all in obtaining the exact value of this integral, no matter how close the source point is to the element.

2.2 Evaluate the regularized nearly-singular integral by nonlinear transformation

The order of the first integral on the right hand side of (6), i.e.,

$$\int_{\Delta L} T_{ij}(P, P_0) [u_j(P) - u_j(P'_0)] dL(P)$$

is weakened to $O(r')$ $O(r)$. However, as r' is not equal to r , near singularity in the above integral is not canceled completely and ordinary Gauss quadrature is not good enough to evaluate it accurately when e is in micro- or nano-scale. For simplicity, during the following discussion we use the natural coordinate system $\xi \in [-1, 1]$ and the coordinate ξ of P'_0 is 0 as shown in Fig. 4. Then in the natural coordinate system, r and r' can be written as:

$$r' = \xi, \quad r = \sqrt{\xi^2 + e^2} \quad (12)$$

where e is the distance from source P_0 to the element ΔL . For simplicity and clarity, the following integral is discussed at this time

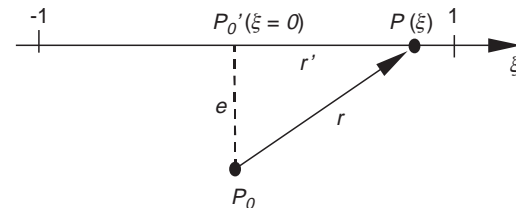


Fig. 4. Distances r and r' in the natural coordinate system

$$\begin{aligned}
\int_{\Delta L} \frac{r'}{r} dL &= \int_{-1}^1 \sqrt{\frac{\xi^2}{\xi^2 + e^2}} d\xi \\
&= \int_{-1}^0 \sqrt{\frac{\xi^2}{\xi^2 + e^2}} d\xi + \int_0^1 \sqrt{\frac{\xi^2}{\xi^2 + e^2}} d\xi \\
&= 2 \int_0^1 \sqrt{\frac{\xi^2}{\xi^2 + e^2}} d\xi. \tag{13}
\end{aligned}$$

The above integral can not be evaluated accurately by ordinary Gauss quadrature when e^2 is small, say $e^2 = 10^{-2}$ to 10^{-5} (but not zero), and nonlinear coordinate transformation is needed. We can see this by considering the following three functions in the form:

$$y = C \sqrt{\frac{\xi^m}{\xi^n + e^2}}. \tag{14}$$

We select,

$$y_1 = 2 \sqrt{\frac{\xi^2}{\xi^2 + 10^{-5}}}, \quad (m = 2, n = 2, e^2 = 10^{-5})$$

$$y_2 = 2 \sqrt{\frac{\xi^2}{\xi^2 + 1}}, \quad (m = 2, n = 2, e^2 = 1)$$

$$y_3 = 4 \sqrt{\frac{\xi^6}{\xi^4 + 10^{-5}}}, \quad (m = 6, n = 4, e^2 = 10^{-5})$$

where the y_1, y_2 are the function in integral (13) with $e^2 = 10^{-5}$ and 1, respectively, and y_3 with $e^2 = 10^{-5}$ and higher orders of ξ .

Figure 5 is a plot of the three functions in the range of $\xi \in [0, 1]$. It is found that, in the neighborhood of zero, y_1 changes very rapidly, while y_2 and y_3 vary moderately. When approximating the above three functions by polynomials, we will find that higher order polynomials should be used for function y_1 , which means higher order Gauss quadrature is needed when evaluating its integration. A lower order of Gauss quadrature may be used for y_1 if we

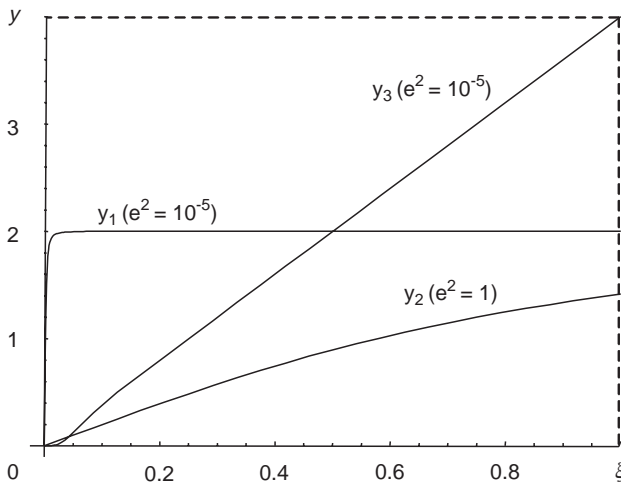


Fig. 5. Plot of the functions y_1, y_2 and y_3

can somehow reduce its rate of variation in the neighborhood of zero. There are two possible ways to realize this. One way is to increase the absolute value of e^2 so that y_1 will behave more like y_2 . However, this approach is infeasible since the absolute value of e is decided by the location of source P_0 and element ΔL and it can not be changed. The other way is to increase the order of ξ in the denominator so that y_1 will behave more like y_3 . This can be achieved by using the following *nonlinear coordinate transformation*.

Let $\xi = \eta^2$ in integral (13). Then (13) is transformed to:

$$\begin{aligned}
2 \int_0^1 \sqrt{\frac{\xi^2}{\xi^2 + e^2}} d\xi &= 4 \int_0^1 \eta \sqrt{\frac{\eta^4}{\eta^4 + e^2}} d\eta \\
&= 4 \int_0^1 \sqrt{\frac{\eta^6}{\eta^4 + e^2}} d\eta. \tag{15}
\end{aligned}$$

We find that for the special case $e^2 = 10^{-5}$, the function in the integral (13) changes from y_1 to y_3 . With the order of ξ in the denominator increasing from 2 to 4, the rate of change of y_3 in the neighborhood of zero is reduced greatly, Fig. 5. It is much easier to evaluate y_3 accurately by using a smaller number of Gauss points.

In the above discussion, we considered the singular part $1/r$ in the stress kernel T_{ij} and r' part in $u_j(P) - u_j(P'_0)$ only. It is true that for this simplified case, an order of two nonlinear transformation in (15) is enough to evaluate the integral accurately even if the absolute value of e^2 is small. However, when the first integral in the right hand side of (6) is evaluated, for the influence from other parts of T_{ij} and $u_j(P) - u_j(P'_0)$, higher order transformation as follows may be needed.

Let $\xi = \eta^m (m > 2)$ in (13), thus (13) is transformed to:

$$\begin{aligned}
2 \int_0^1 \sqrt{\frac{\xi^2}{\xi^2 + e^2}} d\xi &= 2 \int_0^1 m \eta^{m-1} \sqrt{\frac{\eta^{2m}}{\eta^{2m} + e^2}} d\eta \\
&= 2 \int_0^1 m \sqrt{\frac{\eta^{4m-2}}{\eta^{2m} + e^2}} d\eta,
\end{aligned}$$

where m is called the order of the nonlinear coordinate transformation. We observe that, when m is large enough, the first integral on the right hand side of (6) can be evaluated accurately. From our experience, for quadratic elements, when e is on 10^{-6} scale or smaller, $m = 6$ will be accurate enough. But best results will be obtained when m is between 12 and 14 using 10–20 Gauss points.

Several other important points for nonlinear coordinate transformation deserve mention:

- (1) The nonlinear coordinate transformation can be used for any type of elements, e.g., linear, quadratic or cubic elements (quadratic elements are used in the example problems in this paper).
- (2) No CPU time penalty is incurred in using this nonlinear coordinate transformation, because all values of η^m at the Gaussian points can be evaluated once before the kernels are computed.

- (3) The regularization process in part (2.A) is indispensable, because it significantly reduces the order of singularity and provides the basis for the success of the nonlinear coordinate transformation.
- (4) Although in the mathematical sense, larger m should be better, m should not be greater than 16, where the value of η^m ($-1 \leq \eta \leq 1$) may approach zeros within the machine precision.

2.3 Evaluation of nearly weakly-singular integral

In 2-D elasticity problems, the weakly-singular integrals given in (4) contain the singular term $\ln(r)$. In the singular case, i.e., if $r = 0$, a special logarithm Gaussian quadrature can be employed. However, when r is very small but not zero, this nearly weakly-singular integral can cause difficulties in the 2-D BEM procedure. Attempts have been made to obtain the analytical expressions for this integral with the weakly-singular kernel when $r \neq 0$, but they are successful only for constant and linear elements. For general curved elements, such as quadratic elements, a more general approach needs to be established. Here we use a similar nonlinear coordinate transformation as developed in the previous section to evaluate the nearly weakly-singular integrals accurately, no matter how close the source point is to the element of integration. To illustrate the idea, let us consider the natural coordinate system ξ again and use the nonlinear coordinate transformation $\xi = \eta^m$ (the approach is equally applicable to any types of elements on which the local coordinate system ξ can always be established). We obtain:

$$\begin{aligned} \int_{\Delta L} \ln(r) dL &= 2 \int_0^1 \frac{1}{2} \ln(\xi^2 + e^2) d\xi \\ &= \int_0^1 m \eta^{m-1} \ln(\eta^{2m} + e^2) d\eta. \end{aligned}$$

For a similar reason to that given in section (2.2), this integral can be evaluated accurately using a small number of Gauss points when m is large enough, as revealed in the numerical studies.

3 Numerical verification

To verify the method developed above, three simple test problems are studied in which BEM solutions are compared with the exact or FEM solutions.

3.1 Test problem 1: a thin plate

First, a thin plate under external pressure p shown in Fig. 6 is studied. We assume the length of the plate in z direction

is large so that this problem can be simplified as a plane strain problem. The length L of the plate in x direction is constant in this study, while the thickness h changes from L to $10^{-9} L$. Note that the thickness is changing from macro-scale to micro-scale, and eventually to nano-scale, which may already be outside of the limits of the continuum mechanics assumptions for many materials. However, it is of more interest here to verify the validity and effectiveness of the developed BEM approach for such 2-D thin structures.

In the BEM model, the boundary of the plate is discretized with only *four* quadratic boundary elements, two elements with length $L = 4$ m, and two other elements with size (thickness h) changing from L to $10^{-9} L$, as shown in Fig. 6. On node 1 and 3, displacement in y direction is constrained. On node 2, displacement components in both x and y directions are constrained. Figure 7 shows the displacement of node 5 in x direction by the BEM without using singular subtraction and the nonlinear coordinate transformation. It is obvious that the results deteriorate quickly as the thickness decreases. Figure 8 shows the same displacement results by the BEM with the singularity subtraction and nonlinear coordinate transformation. We see that even for thickness to length ratio h/L in the nano-scale, results are still very good. Results for the stress components are even more accurate for this example, almost reproducing the exact values (e.g., $\sigma_y = 7.5$ Pa) for all the values of the thickness. This proves that the developed analytical work in the BEM procedure is effective. The finite element analysis of this simple problem was also attempted, but it was soon found out that the number of the 2-D finite elements were so large that the task quickly exceed the capacity of the computer used. A simple calculation reveals that the total number of the 2-D finite elements required for this example is determined by

$$M = 2 \times \frac{L}{\left(5 \times \frac{h}{2}\right)} = \frac{4L}{5h},$$

if only two layers of elements are used across the thickness and an aspect ratio of five is maintained. This gives $M = 3,200,000$ elements if $h = 10^{-6}$ m ($L = 4$ m) and an even larger number of nodes, depending on the type of finite elements employed.

The example problem studied here is a very simple one in thin structures. The purpose of using this example is to verify the correctness of the singularity subtraction and nonlinear coordinate transformation in dealing with nearly-singular integrals. Because of the simplicity of the boundary condition (constant pressure), a model with much smaller length can actually be applied. For example, in the cases when thickness of the plate is in the micro-

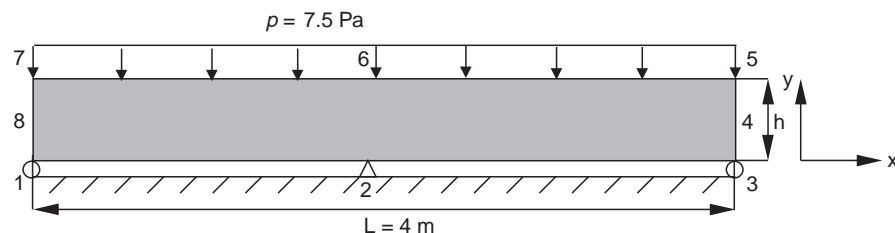


Fig. 6. A thin plate under constant pressure p (2-D plain strain model, shear modulus $\mu = 8.0 \times 10^{10}$ Pa, Poisson's ratio $\nu = 0.2$)

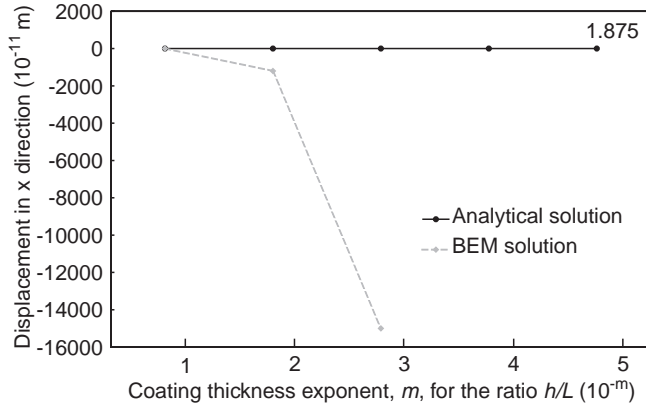


Fig. 7. The displacement of node 5 in x direction when singularity subtraction and nonlinear transformation are not used

scale, we can use a model with length in the micro-scale. Then, no nearly singular integral problem exists in the BEM. Also no aspect ratio problem exists for FEM using 2-D elements. However, more cases exist that the length of the model can not be decreased. For example, in this simple problem if the pressure p is not constant but varies along the side of the plate, then the model with length = 4 m should be used. In such situation, with the 2-D BEM, as we have seen in this example, accurate results can be obtained by using just a few boundary elements.

3.2 Test problem 2: thin coating on a shaft

The method developed in this paper will be used to solve two related sample problems of a shaft with a thin coating. Plane strain is assumed, and the shaft is considered to be rigid when compared to the coating. The shaft and coating have outer radii r_s and r_c respectively, and the two cases to be considered are: (a) the coating is of uniform thickness $h = r_c - r_s$ as shown in Fig. 9(a), and (b) the coating is of nonuniform thickness; both the shaft and coating profiles remain circular, but their centers are misaligned, producing some normalized eccentricity $\delta = \frac{x_c}{r_c - r_s}$, where x_c is the center offset, as shown in Fig. 9(b). In both examples, the coated system is loaded by a pressure p which is

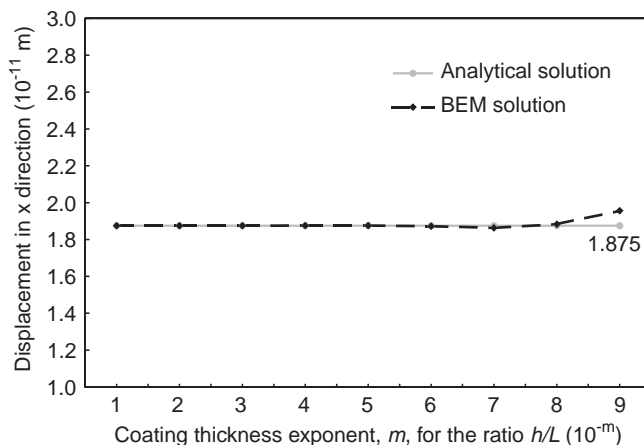


Fig. 8. The displacement of node 5 in x direction when singularity subtraction and nonlinear transformation are used

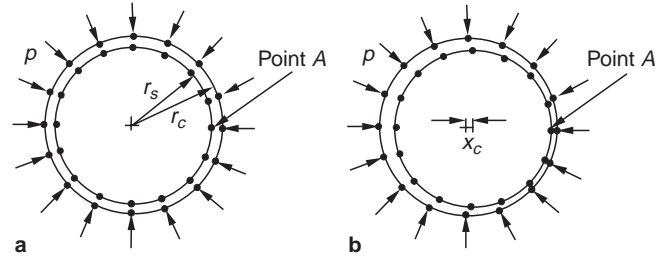


Fig. 9. Cross section of a shaft with coatings of a uniform and b nonuniform thickness

uniformly distributed around the circumference. In addition, the boundary conditions for both cases, considering the rigid shaft assumption, are $u_x = u_y = 0$ for all nodes at the shaft/coating interface. Finally, the BEM discretization uses 16 elements for both sample problems, regardless of the thickness of the structure. The FEM discretization varies according to the structure thickness and element aspect ratio requirements.

(a) First case: uniform thickness coating

For the uniform thickness case, an analytical solution for the stress field can be obtained (Boresi and Chong 1987), and a comparison of BEM and FEM solutions can be made. For this problem, the coating thickness varies in the range of $10^{-2}r_s \leq h \leq 10^{-9}r_s$; this variation is achieved by holding the shaft radius r_s constant while varying the coating outer radius r_c appropriately. The stress solution has been obtained by the BEM and compared with the analytical solution.

Figure 10 shows the error magnitude of radial stress σ_{rr} prediction using the BEM for the uniform coating thickness. Note that as the coating thickness decreases, no loss in solution accuracy is shown. In fact, in this particular case, the solution becomes better as the thickness gets smaller. The radial stress approaches the applied pressure p , as expected, when the thickness approaches zero.

(b) Second case: nonuniform thickness coating

The second important case for analysis is the nonuniform thickness case, which does not demonstrate the symmetry of the first sample problem. As a result, the FEM mesh in this case must consider the entire structure, which significantly increases the number of elements. In addition, as the eccentricity δ increases, more finite elements are required in the thinnest section in order to maintain reasonable element aspect ratio. Note that the same BEM mesh is used, including 16 elements. While no analytical solution exists for $\delta \neq 0$ case, the asymptotic behavior of the solution as $\delta \rightarrow 0$ can be checked to verify the formulation. In this case, shaft radius is held constant at $r_s = 0.1$ m and coating outer radius is also held constant at $r_c = 0.11$ m. However, the eccentricity has been systematically varied over the entire range $0 \leq \delta < 1$. For each case of eccentricity, the stress solution has been obtained by using the BEM, while the FEM solution breaks down as $\delta \rightarrow 1$.

Figure 11 shows the normalized radial stress σ_{rr} at point A, and also the number of nodes needed to achieve solu-

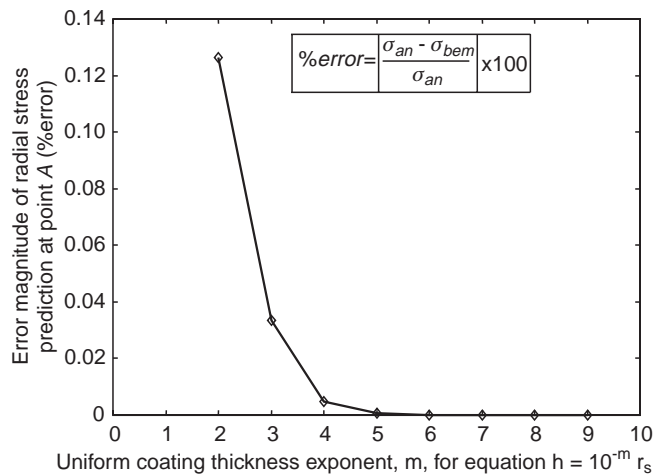


Fig. 10. Error magnitude of the BEM radial stress prediction for uniform coating thickness

tion for both the BEM and FEM. Note first the asymptotic behavior of the BEM solution, which approaches the analytical value of the sample problem as $\delta \rightarrow 0$ (case (a)). Also notice that the same stress value at point A approaches the applied pressure p as $\delta \rightarrow 1$, which is consistent with the physical interpretation. Again, the BEM mesh does not change across the entire range of normalized eccentricity. The solution time and memory requirements are therefore quite modest for the BEM procedure. The FEM solution, however, demonstrates a very different behavior. While the low eccentricity cases are easily solved with the FEM, with a fairly small number of elements, the solution requires significantly more effort for $\delta \rightarrow 1$. The FEM element count increases dramatically at approximately $\delta = 0.9$, corresponding to an absolute coating thickness of $h = 0.001$ m at the thinnest point on the structure. Indeed, for $\delta > 0.99$, the FEM solution becomes infeasible due to memory limitations. On the other hand, the BEM can continue to provide results for $\delta = 0.999, 0.9999$ and 0.99999 without any difficulty, because of the effective approach developed in this paper to deal with the nearly-singular integrals. Clearly, the BEM

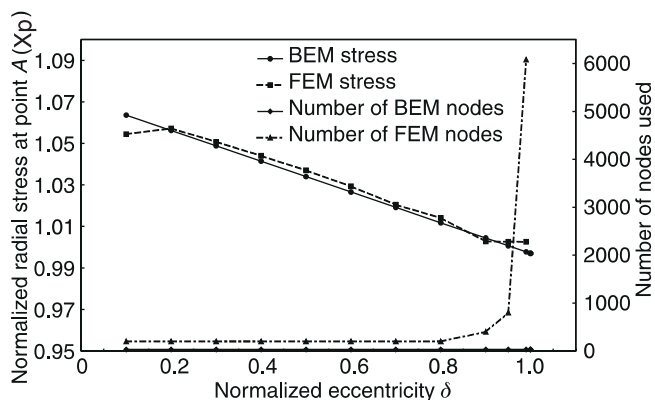


Fig. 11. Radial stress prediction and numbers of nodes required for nonuniform coating thickness (Note that the highest normalized eccentricity solved is: $\delta = 0.99999$ for BEM and $\delta = 0.99$ for FEM)

solution, which does not require a refined mesh, regardless of the coating thickness, is preferable.

4 Discussion

The applicability of the conventional BIE for 2-D elasticity problems to the analysis of 2-D thin structures in micro- and nano-scale is investigated in this paper. It is shown that the CBIE, using singularity subtraction and nonlinear coordinate transformation to deal with the nearly singular integrals, will be very accurate and efficient in modeling 2-D thin structures. The numerical verification on two sample problems using thin coating models supports this assertion.

For all the test problems of thin structures studied in this paper, the BEM provides a computationally-efficient solution for both displacement and stress fields. While the FEM performs well over certain parameter ranges, in general it is not suitable for thin structures such as those in the examples for the following reasons: (1) For accurate stress solution using FEM, particularly for thin structures in which normal stresses are of interest, 2-D continuum elements must be used. Shell elements cannot be used because they lack accuracy in stress predictions, a crucial consideration in many thin structure problems including fatigue performance of coated machine elements. As a result, for the required 2-D quadratic plane strain elements, the number of degrees of freedom increases rapidly with the number of elements. In addition, shell elements present implementation problems for structures of non-uniform thickness, for which each shell element would possess a different thickness. (2) Finite element count increases rapidly for thin structures due to aspect ratio limitations. To maintain element aspect ratio for the nonuniform thickness case, a large number of elements must be inserted in the thinnest portion of the structure. In addition, for each change in thickness, a complete remeshing of that portion of the domain must be conducted to insure accurate solution. (3) The FEM eventually becomes infeasible due to memory constraints and the necessity for a very large number of DOF's for very thin structural problems, or for cases in which symmetry cannot be exploited.

The BEM is able to circumvent these problems through the novel approach developed in this paper. The BEM approach to thin structure analysis described here can solve the stress field problem accurately for (in theory) arbitrarily thin structures, because of the following attractive features: (1) Using only boundary discretization (e.g., quadratic line elements) instead of domain discretization (area elements), the BEM does not suffer from thickness or aspect ratio difficulties related to FEM shell or 2-D continuum elements described above. (2) Therefore, the element count using the BEM can be held constant for thin structural problems as described in the example, without any loss in solution accuracy as the thickness decreases. (3) The BEM procedure therefore requires no remeshing as the thickness decreases. The BEM solution seldom confronts memory or storage issues in the numerical solution, and symmetry issues need not be considered.

Using the analytical singularity subtraction and non-linear coordinate transformation techniques demonstrated in this paper, the seemingly difficult task of evaluating the nearly-singular integrals in the BIE for 2-D thin structures can be dealt with effectively and efficiently. The BEM approach developed here for thin structural problems achieves accurate stress predictions for arbitrarily thin structures, even for problems with geometric length scale approaching the limits of the validity of continuum mechanics formulations.

The developed method of using the BEM based on elasticity theory for analyzing 2-D thin structures can be extended readily to model layered coatings, thin films or other layered structures to analyze contact stresses, interfacial cracks, thermal effects and nonlinear deformations. All of these topics, in the cases of bulky structures, can be dealt with effectively and efficiently by the BEM (Mukherjee 1982; Cruse 1988; Banerjee 1994). Some work along this line for thin structures is already underway.

5

Conclusion

An efficient way to deal with nearly singular integrals in 2-D elastostatic BEM is developed in this paper. By using the singularity subtraction and nonlinear transformation, nearly singular integrals in 2-D BEM can be evaluated accurately, even if the ratio of the distance to the typical element size is smaller than the order of 10^{-6} . This BEM approach will be most useful in the numerical analysis of thin structures such as coating system or thin films on micro and even smaller scales where other computational models, such as the FEM, become inefficient or fail.

References

- Banerjee, P. K. (1994). *The boundary element methods in engineering*. New York, McGraw-Hill
- Bhushan, B.; Gupta, B. K. (1991). *Handbook of tribology: materials, coatings, and surface treatments*. New York, McGraw-Hill
- Boresi, A. P.; Chong, K. P. (1987). *Elasticity in Engineering Mechanics*. New York, Elsevier
- Chien, C. C., Rajiyah, H., Atluri, S. N. (1991). "On the evaluation of hyper-singular integrals arising in the boundary element method for linear elasticity." *Computational Mechanics*, 8: 57-70
- Cruse, T. A. (1988). *Boundary Element Analysis in Computational Fracture Mechanics*. Dordrecht, Boston, Kluwer Academic Publishers
- Cruse, T. A. (1996). "BIE fracture mechanics analysis: 25 years of developments." *Computational Mechanics* 18: 1-11
- Cruse, T. A.; Aithal, R. (1993). "Non-singular boundary integral equation implementation." *International Journal for Numerical Methods in Engineering* 36: 237-254
- Gray, L. J.; Martha, L. F.; Ingrassia, A. R. (1990). "Hypersingular integrals in boundary element fracture analysis." *International Journal for Numerical Methods in Engineering* 29: 1135-1158
- Huang, Q.; Cruse, T. A. (1993). "Some notes on singular integral techniques in boundary element analysis." *International Journal for Numerical Methods in Engineering* 36: 2643-2659
- Kreyszig, E. (1972). *Advanced Engineering Mathematics*. New York, John Wiley and Sons, Inc
- Krishnasamy, G.; Rizzo, F. J.; Liu, Y. J. (1994). "Boundary integral equations for thin bodies." *International Journal for Numerical Methods in Engineering* 37: 107-121
- Krishnasamy, G.; Rizzo, F. J.; Rudolph, T. J. (1991). "Hyper singular boundary integral equations: their occurrence, interpretation, regularization and computation." *In: Developments in Boundary Element Methods VII*. Eds. P. K. Banerjee and et al., London, Elsevier Applied Science Publishers. Chapter 7
- Liu, Y. J. (1998). "Analysis of shell-like structures by the boundary element method based on 3-D elasticity: formulation and verification." *International Journal for Numerical Methods in Engineering* 41: 541-558
- Liu, Y. J.; Rizzo, F. J. (1997). "Scattering of elastic waves from thin shapes in three dimensions using the composite boundary integral equation formulation." *Journal of the Acoustical Society America* 102 (2) (Pt. 1, August): 926-932
- Liu, Y. J.; Zhang, D.; Rizzo, F. J. (1993). "Nearly singular and hypersingular integrals in the boundary element method." *In: Boundary Elements XV*, Worcester, MA, Computational Mechanics Publications. 453-468
- Mukherjee, S. (1982). *Boundary Element Methods in Creep and Fracture*. New York, Applied Science Publishers
- Richardson, J. D., Cruse, T. A., Huang, Q. (1997). "On the validity of conforming BEM algorithms for hypersingular boundary integral equations." *Computational Mechanics*, 20: 213-220
- Subramanian, C.; Strafford, K. N. (1993). "Review of multicomponent and multilayer coatings for tribological applications." *Wear*: 85-95